Int J Thermophys (2012) 33:1808–1813
DOI 10.1007/s10765-012-1286-x

Study of Tissue Phantoms, Tissues, and Contrast Agent with the Biophotoacoustic Radar and Comparison to Ultrasound Imaging for Deep Subsurface Imaging

R. Alwi · S. Telenkov · A. Mandelis · F. Gu

Received: 10 February 2012 / Accepted: 14 August 2012 / Published online: 5 September 2012

Abstract In this study, the imaging capability of our wide-spectrum frequency-domain photoacoustic (FD-PA) imaging *alias* "photoacoustic radar" methodology for imaging of soft tissues is explored. A practical application of the mathematical correlation processing method with relatively long (1 ms) frequency-modulated optical excitation is demonstrated for reconstruction of the spatial location of the PA sources. Image comparison with ultrasound (US) modality was investigated to see the complementarity between the two techniques. The obtained results with a phased array probe on tissue phantoms and their comparison to US images demonstrated that the FD-PA technique has strong potential for deep subsurface imaging with excellent contrast and high signal-to-noise ratio. FD-PA images of blood vessels in a human wrist and an *in vivo* subcutaneous tumor in a rat model are presented. As in other imaging modalities, the employment of contrast agents is desirable to improve the capability of medical diagnostics. Therefore, this study also evaluated and characterized the use of Food and Drug Administration (FDA)-approved superparamagnetic iron oxide nanoparticles (SPION) as PA contrast agents.

Keywords Contrast agent · Frequency domain · Photoacoustic radar · SPION · Tissue phantom · Ultrasound

R. Alwi · S. Telenkov · A. Mandelis (✉)
Center for Advanced Diffusion-Wave Technologies (CADIFT), Department of Mechanical Engineering, University of Toronto, 5 King's College Road, Toronto, ON M5S 3G8, Canada
e-mail: mandelis@mie.utoronto.ca

F. Gu
Department of Chemical Engineering, University of Waterloo, 200 University Avenue West, Waterloo, ON N2L 3G1, Canada

1 Introduction

The field of biomedical photoacoustic (PA) imaging has been growing significantly over the past decade [1] where pulse lasers have been the standard choices for optical excitation. Although nanosecond high-peak laser excitations can provide strong acoustic responses and adequate signal-to-noise ratio (SNR), those pulsed-PA systems tend to be bulky, expensive, and not flexible enough in wavelength tuning, and require qualified personnel for consistent system performance, factors which may eventually make them hard to implement clinically. We have introduced [2–4] an alternative PA technique using a relatively low-power intensity-modulated continuous wave (CW) laser as the optical source and have developed it to the extent capable of competing well with the pulsed-PA systems in terms of SNR, spatial resolution, and depth detectivity [5,6]. A wide availability of compact and relatively inexpensive fiber or diode lasers in the near-infrared (NIR) spectrum makes the prospect of portable and efficient PA modalities for clinical use very appealing. With a frequency-sweep (chirp) modulation and a cross-correlation processing commonly employed in radar technology [7], the chirped CW laser-based frequency-domain PA system is also referred to as "the PA radar" [8] to emphasize the preferential role of the frequency spectrum in signal processing.

The laser PA method of tumor detection relies on light absorption by the concentrated blood in the tumor angiogenesis network [9,10]. The received optically induced acoustic waves are used to determine the vasculature location and the oxygen saturation of blood, taking advantage of the unique spectral signatures of oxy- and deoxy-hemoglobin absorption [11,12]. In tumor screening by ultrasound (US) or X-ray mammography, early-stage tumors are not easily detectable because the mechanical contrast or the density delineation of tumor boundaries is not significant. Nevertheless, that kind of limitation should not be the case for optical-contrast-based diagnostic modalities, such as PA imaging.

In this study, tissue phantoms resembling human tissues in their optical and acoustical properties [13] and simulating early-stage tumor environment were used to systematically test and optimize the capability of our frequency-domain photoacoustic (FD-PA) phased array imaging in a controlled way with regard to biomedical applications. A PA image comparison with US images was investigated to confirm the complementarity between the two techniques. PA radar images of blood vessels in a human wrist and *in vivo* subcutaneous tumor detection in a rat xenograft model are presented. In addition, we also evaluated silica-coated super paramagnetic iron oxide (Fe_3O_4) nanoparticles (SPION) as a potential PA contrast enhancer. SPION is a well-established contrast agent in magnetic resonance imaging (MRI), Food and Drug Administration (FDA) approved, and has excellent safety profile for clinical use [14].

2 Experimental Apparatus and Procedures

Detailed descriptions of the PA radar technique signal processing under chirped laser excitation are given elsewhere [4]. The PA radar experimental setup is shown in Fig. 1. The 1064 nm CW laser (IPG Photonics, Boston, MA) output was intensity-modulated

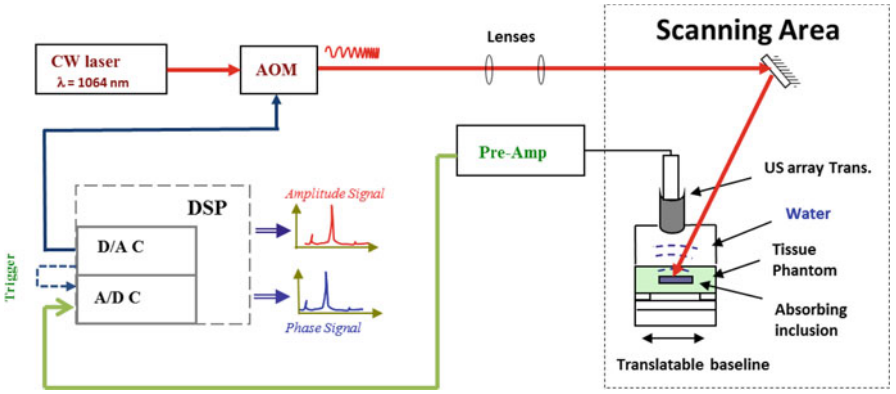

Fig. 1 Experimental setup of PA radar measurements

using an acousto-optic modulator (AOM; Neos Technologies, FL) to produce periodic PA waves. A 1 ms duration sinusoidal chirp waveform with a 1 MHz to 5 MHz frequency sweep was synthesized using a LabVIEW© program and uploaded to the function generator (PXI-5442; National Instrument, Austin, TX) also used for data-acquisition synchronization. Two lenses were positioned so as to form a 3 mm beam diameter. A transparent and cylindrical acrylic water-filled container with open ends, the bottom part sealed with a thin plastic film, was used for acoustic coupling. Two detection schemes were used for the present experiments. For phantom and human blood vessel imaging, the acoustic detector was a standard 64 element 3.5 MHz phased array transducer (GE Parallel Design Inc., Phoenix, AZ) with an 80 % mean bandwidth at −6 dB and 0.254 mm pitch [15]. Detected array signals were pre-amplified and sent to a multiplexer board (NI PXI-2593) before being fed to a modular eight-channel analog-to-digital converter (ADC; PXI-5105). For the presented tumor imaging result and SPION detection, we used a single-element 3.5 MHz focused transducer ($f = 25.4$ mm; Panametrics v382, Olympus NDT Inc., Waltham, MA) and the pre-amplified signals were transferred directly to an ADC (PXI-5122). A 1 W power laser irradiance incident on the samples was kept constant throughout the experiments, and an averaging of (100 to 1000) chirps was employed to increase the SNR.

A tissue phantom (reduced scattering coefficient: $\mu_s' = 4\,\mathrm{cm}^{-1}$) with an absorbing rectangular inclusion (absorption coefficient: $\mu_a = 2\,\mathrm{cm}^{-1}$, $\mu_s' = 4\,\mathrm{cm}^{-1}$, size $10 \times 10 \times 6\,\mathrm{mm}^3$) located 12 mm to 15 mm below the surface and made of the same polyvinyl chloride plastisol (PVCP) was fabricated [13] to simulate an early-stage tumor. A female immunodeficient rat (Charles River, Wilmington, MA) bearing a subcutaneous hyphopharingeal FaDu tumor in its thigh was used for the *in vivo* animal imaging. The animal experiment was conducted under the animal use protocol approved by the University of Toronto. For the PA contrast agent preparation, SPION with an 8 nm diameter iron oxide core were synthesized by a co-precipitation method [16] and coated with 3 nm thickness of silicon dioxide [17].

3 Results

Figure 2a, b shows the FD-PA and US images, respectively, and their comparison on the early-tumor-detection scheme performed in the PVCP tissue phantom. The inclusion in the US image (a dashed rectangle) was barely visible due to lack of mechanical contrast with surrounding material. Therefore, the acoustic reflection was negligible and insufficient to provide adequate image contrast. On the other hand, the FD-PA correlation image strongly indicated the presence of the inclusion at a depth of 12 mm to 15 mm below the surface. In the PA image, a small bright spot on the surface was due to the laser irradiance incident on the phantom. Since the light was dispersed in the scattering medium, the broadened beam reaching the inclusion resulted in a wider PA area coverage of the inclusion. The reconstructed sector image of a human wrist as shown in Fig. 2c, reveals discrete bright spots related to the PA signals generated by near-surface blood vessels. Due to the limitation of the axial resolution of the 3.5 MHz phased array transducer, the locations of subcutaneous blood vessels were not resolvable from the skin surface in the reconstructed PA radar image. The laser beam incident on the tissue surface was maintained at the safety level [18] during data acquisition.

In vivo detection of the subcutaneous tumor in the thigh of the female rat model and its PA and US image comparison are shown in Fig. 3. By translating the single-element 3.5 MHz transducer and the incident beam concomitantly, we obtained two-dimensional PA images of a healthy (Fig. 3a) and tumor (Fig. 3b) regions of the thigh to showcase their endogenous contrast difference. An US scan (Fig. 3c) using a 128 element 7.5 MHz linear array transducer (GE Parallel Design Inc., Phoenix, AZ) over the same tumor region as in Fig. 3b was performed. The thickness of the subcutaneous tumor was found to be ∼1 cm by both PA and US images. Our PA radar system shows good correlation with the US imaging modality to estimate the size and shape of the subcutaneous tumor. The fact that only front and back tumor surfaces appear delineated in the PA image (Fig. 3b) is consistent with our theoretical simulations of the PA signal generated in a solid absorbing region with a fixed or continuously variable optical absorption coefficient [19].

PA detection of the silica-coated SPION up to ∼9 mm and ∼24 mm inside a tissue-like intralipid solution (Intralipid® 20 %, Fresenius Kabi AB, Upsala, Sweden;

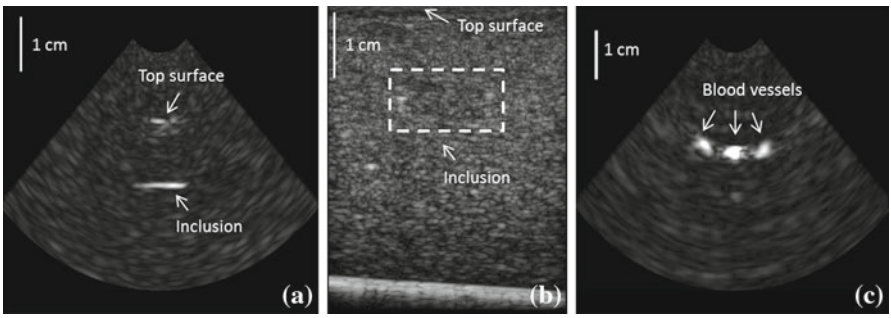

Fig. 2 PA (a) radar and (b) ultrasound (US) images on the detection of an early-tumor-like subsurface inclusion inside the PVCP phantom. (c) PA radar image of discrete blood vessels in a human wrist

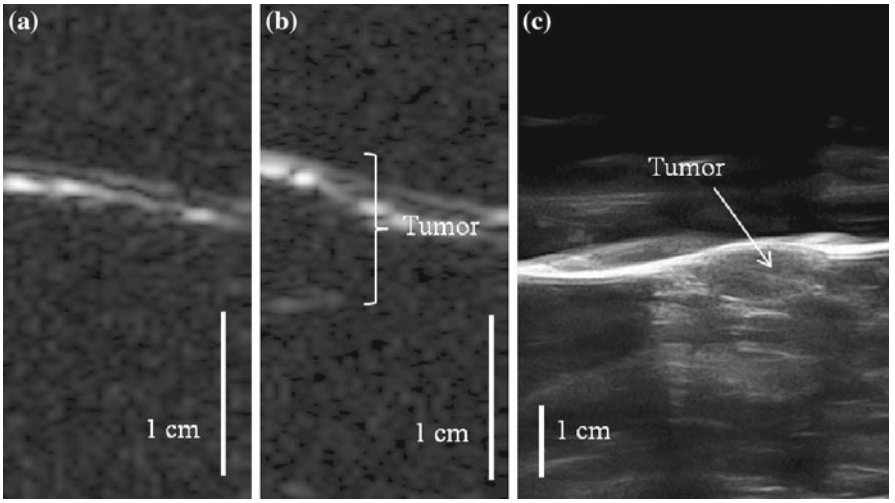

Fig. 3 Comparison of PA radar and US images of an *in vivo* subcutaneous tumor. PA scans over (a) normal skin and (b) the subcutaneous tumor region of a rat thigh. (c) US scan over the same tumor area as (b)

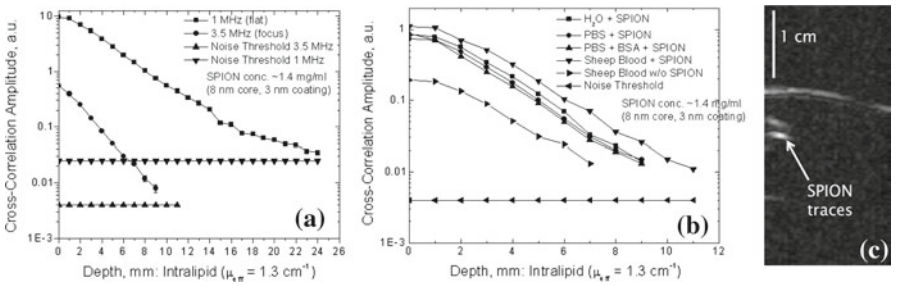

Fig. 4 (a) Maximum depth detection determination of the silica-coated SPION inside the intralipid solution. (b) Effect of different solvents on the silica-coated SPION-generated PA signal. (c) PA radar image of silica-coated SPION inside an *ex vivo* rat thigh. Detection was effected either using the single-element 3.5 MHz focused transducer; or as specified in the inset. H_2O = water; *PBS* phosphate buffer saline; *BSA* bovine serum albumin

effective optical attenuation coefficient: $\mu_{\text{eff}} = 1.3\,\text{cm}^{-1}$) using a single-element 3.5 MHz focused and a 1 MHz unfocused (Panametric A303S) transducer, respectively, as shown in Fig. 4a, demonstrates the nanoparticle potential as a PA contrast enhancer. With the trade-off between axial resolution and attainable imaging depth, our previous study [5] has shown that using a low frequency transducer could increase the FD-PA imaging depth significantly. Figure 4b, measured using the single-element 3.5 MHz focused transducer, shows that the silica-coated SPION were optically stable under different solvents such as phosphate buffer saline (PBS) and bodily fluids (e.g., bovine serum albumin (BSA) and sheep blood). In addition, the PA depth detection of the mixture of silica-coated SPION and sheep blood (▼ line) was increased ∼1.5-fold over the detection threshold of pure sheep blood (► line). A 2D image of the SPION

detection inside an *ex vivo* rat thigh, which was obtained by translating the 3.5 MHz focused transducer, is presented in Fig. 4c.

4 Conclusions

We have demonstrated the imaging capability of our PA radar technique with frequency-swept optical excitation and cross-correlation signal processing, using both single-element and phased array transducers on tissues and tissue phantoms. The complementarity between the PA and US systems has been confirmed through image comparison. We have examined and shown the potential of silica-coated SPION as PA contrast agents.

Acknowledgments This work was supported by the Natural Sciences and Engineering Research Council (NSERC) through Discovery and Strategic grants; by the Premier's Discovery Award in Science and Technology, Ministry of Research and Innovation (MRI), Ontario; by a CFI-ORF Grant; and by the Canada Research Chairs Program.

References

1. P. Beard, Interface Focus **1**, 602 (2011)
2. Y. Fan, A. Mandelis, G. Spirou, I.A. Vitkin, J. Acoust. Soc. Am. **116**, 3523 (2004)
3. S.A. Telenkov, A. Mandelis, J. Biomed. Opt. **11**, 044006 (2006)
4. S. Telenkov, A. Mandelis, B. Lashkari, M. Forcht, J. Appl. Phys. **105**, 102029 (2009)
5. S.A. Telenkov, A. Mandelis, J. Biomed Opt. **14**, 044025 (2009)
6. B. Lashkari, A. Mandelis, Rev. Sci. Instrum. **82**, 094903 (2011)
7. C.E. Cook, M. Bernfeld, *Radar Signals: An Introduction to Theory and Application* (Artech House, Norwood, MA, 1993)
8. S. Telenkov, A. Mandelis, Proc. SPIE **7899**, 78990Y (2011)
9. S.A. Ermilov, T. Khamapirad, A. Conjustau, M. Leonard, R. Lacewell, K. Mehta, T. Miller, A. Oraevsky, J. Biomed. Opt. **14**, 024007 (2009)
10. J. Jose, S. Manohar, R.G.M. Kolkman, W. Steenbergen, T.G. van Leeuwen, J. Biophotonics **2**, 701 (2009)
11. A. Roggan, M. Friebel, K. Dorschel, A. Hahn, G. Muller, J. Biomed. Opt. **4**, 36 (1999)
12. H.F. Zhang, K. Maslov, G. Stoica, L.V. Wang, Nat. Biotechnol. **24**, 848 (2006)
13. G.M. Spirou, A.A. Oraevsky, I.A. Vitkin, W.M. Whelan, Phys. Med. Bio. **50**, N141 (2005)
14. J.E. Rosen, L. Chan, D.B. Shieh, F.X. Gu, Nanomedicine (2011). doi:10.1016/j.nano.2011.08.017
15. S. Telenkov, R. Alwi, A. Mandelis, A. Worthington, Opt. Lett. **36**, 4560 (2011)
16. F.Y. Cheng, C.H. Su, Y.S. Yang, C.S. Yeh, C.Y. Tsai, C.L. Wu, M.T. Wu, D.B. Shieh, Biomaterials **26**, 729 (2005)
17. B. Luo, X.J. Song, F. Zhang, A. Xia, W.L. Yang, J.H. Hu, C.C. Wang, Langmuir **26**, 1674 (2010)
18. American National Standard, ANSI Z136.1-2007
19. S.A. Telenkov, R. Alwi, A. Mandelis, submitted to Ultrason. Ferroelectr. Freq. Control